Al-Khwarizmi Engineering Journal, Vol. 7, No.4, PP 61 -75 (2011)

Al-Khwarizmi Engineering Journal

Simulation of Oxygen Mass Transfer in an Internal Loop Airlift Reactor with Axial Dispersion Model

Mohammed A. Atiya* **Ameel Mohammed Rahman****
Aseel Abd Al-Jabbar**

**Ministry of Higher Education and Scientific Research/ Research and Development Department*
***Department of Biochemical Engineering/ Al-Khwarizmi College of Engineering/University of Baghdad*

(Received 7 February 2011; Accepted 18 October 2011)

Abstract

The effect of superficial gas velocity within the range 0.01-0.164 m/s on gas holdup (overall, riser and down comer), volumetric oxygen mass transfer coefficient, liquid circulation velocity was studied in an internal loop concentric tubes airlift reactor (working volume 45 liters). It was shown that as the u_{sg} increases the gas holdup and also the liquid circulation velocity increase. Also it was found that increasing superficial gas velocity lead to increase the interfacial area that increases the overall oxygen mass transfer coefficient. The hydrodynamic experimental results were modeled with the available equations in the literature. The predicted data gave an acceptable accuracy with the empirical data.

The final empirical and predicted data were adopted in a mathematical model for oxygen mass transfer to predict the oxygen profile along the reactor. The predicted results have been validated with the experimental results. The simulated results based on the dispersion model for the riser and down comer and the perfect mixed model for the gas-liquid separator, agreed well with the experimental results over the studied range of operating conditions.

Keywords**:** *Airlift bioreactor, reactor, dissolved oxygen; modeling, axial dispersion model, hydrodynamics, mixing, internal loop, liquid circulation velocity, gas holdup.*

1. Introduction

Airlift reactors (ALRs) are pneumatic contactors and have attracted considerable attention compared to the continuous stirred tank reactor (CSTR) due to their simple construction without internal moving parts, high heat and mass transfer capacity, and excellent mixing properties with low power requirements (Guillermo et al., 2009; YuWei, et al., 2008; Chisiti, 1989); and their effectiveness has been proven in numerous applications, including synthesis of methanol or dimethyl ether from synthetic gas, coal liquefaction, Fischer–Tropsch synthesis, petroleum refining, and fermentation systems (Peter et al., 2010; Giovannettonea, et al., 2009; Tongwang et al., 2005; Chisti, 1989).

The hydrodynamic behavior of the gas and liquid flows in airlift reactors is very complicated. The convective and diffusive transfer with volume reactions are realized simultaneously. The convective transfer is a result of a laminar or turbulent (large-scale pulsations) flows. The diffusive transfer is molecular or turbulent (small-scale pulsations). The volume reactions are mass sources as a result of chemical reaction and interphase mass transfer (Chisti, 1989).

An accurate description of the performance of airlift bioreactors is still difficult. One of the most important factors in the operation of airlift reactors is the rate of gas-liquid mass transfer which control the uptake and removal of low soluble components such as oxygen and carbon dioxide.

A number of empirical correlations for estimating mass transfer in terms of the overall mass transfer coefficient (K_la) were available according to various geometrical and operational conditions of the contactor. This parameter is important for the construction of mathematical mass transfer model for the (ALR) as it provides information on the rate at which mass transfer takes place through the

gas-liquid interface. Several mathematical models for mass transfer based on material conservation principals in the ALR have been proposed. These models considered the ALR to be composed of several regions for which mixing characteristics were different. For example, Fields and Slater (1983) showed that, in a concentric tube ALR, gas-liquid separator behaved almost like a perfectly mixed model, whereas the riser and downcomer could be represented by axial dispersion models.

Verlaan (1989) and Merchuk and Yunger (1990) used the plug flow model to represent the flow in the riser and downcomer. These mixing characteristic models were then applied to evaluate mass transfer characteristics in ALR. André et al. (1983) used a tank-in-series model for both riser and downcomer to incorporate backmixing, and the gas separator was considered as a well-mixed region in describing mass transfer in external loop ALR. The same attempts were adopted by Tongwang et al., (2005).

Dhaouadi et al. (2001) proposed the model where gas and liquid flow in riser and downcomer were considered as plug flow but the mixed zones at the separator and the bottom junction were neglected. These literatures showed that oxygen concentration profiles in ALR could be predicted by mathematical models based on material conservation equations.

In general, the plug flow with dispersion is best to describe the behavior of liquid and gas flow in riser, whereas the CSTR model is best to describe the behavior of liquid and gas flow in gas-liquid separator. In the downcomer, there are differences between external loop and internal loop ALR. In external loop ALRs, the interaction between gas and liquid in the downcomer may be neglected without interrupting the predicting capability of the model because there exists very little, if not none, amount of gas in this section. However, this situation is unlikely for internal loop ALRs where a large fraction of gas holdup is usually present in the various sections of the system.

Mathematical models for the internal loop ALR were usually more complicated and subjected to parameter fittings with experimental data. This limits the use of the models to some specific experimental ranges.

This work intends to investigate the accuracy of the mass transfer model developed for the internal loop ALR by assuming the ALR to comprise three interconnecting sections where the interactions between gas and liquid in each section is taken into consideration. To ensure the general use of the model, parameter estimations are performed using independent experiments, and in many cases, they are obtained from other independent sources.

2. Mathematical Model Development

In the present work the mathematical model for the proposed ALR is developed by dividing the whole reactor into three main regions: riser, downcomer and gas separator which is located at the top of the reactor. A mixture of gas and liquid moves from the riser to gas separator. A large fraction of gas bubbles disengages from the system here whilst liquid and the remaining portion of gas move further to the downcomer. In this last section, no gas supply is provided and the fluid content moves downwards and reenters the riser at the bottom of the column together with the inlet gas.

In this proposed mathematical model for the present system, each part of the ALR is considered separately as illustrated in Fig.1. The riser and downcomer are represented by the dispersion model with the exchange of oxygen between gas and liquid phases in each volume element. No liquid is added or removed from the system, whereas gas enters the system only at the bottom section of the riser and leaves the contactor at the gas separator. The behavior of the gas separator is assumed to be well mixed. Hence, the overall model is represented by a series of various types of reactors, i.e. dispersion stirred tank-dispersion.

The following assumptions are considered to simplify the development of this model (Chisti, 1989; Znad et al., 2004):

1. Ideal gas behavior in the system.
2. Isothermal conditions.
3. The effect of hydrostatic head on solubility of oxygen is negligible (for small-scale systems).
4. The overall oxygen volumetric mass transfer coefficient is uniform for all regions in the reactor.
5. The gas holdup is uniform within each individual region.
6. The hydrodynamic parameters, e.g. gas holdups, liquid circulation flowrate, are not a function of time and space.
7. There is no radial effect in the ALR.
8. Oxygen is sparingly soluble in water and Henry's law can be applied to explain the solubility of oxygen in the contactor.

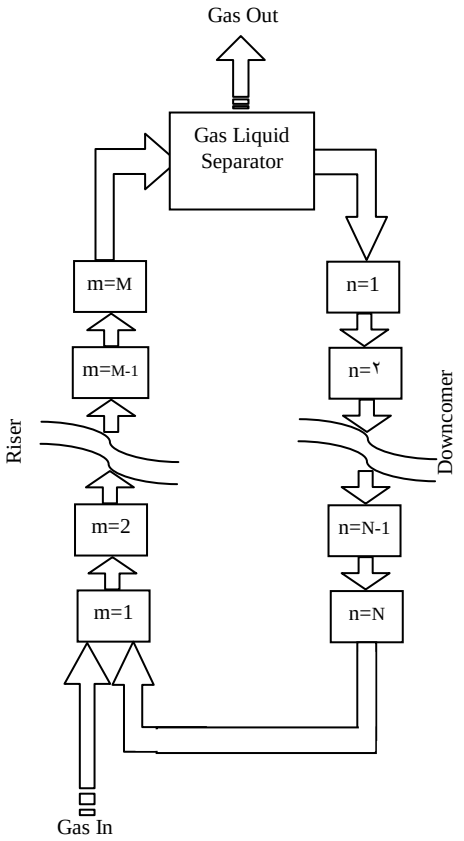

Fig. 1. Schematic Diagram Representing the Internal Loop in the Present ALR.

3. Material balances in ALR regions

The proposed model provides simultaneous differential equations which are material balances of the dissolved oxygen. The unsteady state material balance of dissolved oxygen can be written as follows:

3.1. Riser section

For gas phase oxygen concentration:

At $0 < z_r < L_r$ *:*

$$\frac{\partial O_{g_r}(z_r,t)}{\partial t} = -v_{gr}\frac{\partial O_{g_r}(z_r,t)}{\partial z_r} + D_{gr}\frac{\partial^2 O_{g_r}(z_r,t)}{\partial z_r^2} - \frac{(1-\varepsilon_{gr})}{\varepsilon_{gr}} K_{la}\left(\frac{O_{gr}(z_r,t)}{H} - O_{lr}(z_r,t)\right) \quad \ldots(1)$$

For liquid phase oxygen concentration:

$$\frac{\partial O_{l_r}(z_r,t)}{\partial t} = -v_{gr}\frac{\partial O_{l_r}(z_r,t)}{\partial z_r} + D_{gr}\frac{\partial^2 O_{l_r}(z_r,t)}{\partial z_r^2} + K_{la}\left(\frac{O_{gr}(z_r,t)}{H} - O_{lr}(z_r,t)\right) \quad \ldots(2)$$

3.2. Downcomer section

For gas phase oxygen concentration:

At $0 < z_d < L_d$:

$$\frac{\partial O_{g_d}(z_d,t)}{\partial t} = -v_{gd}\frac{\partial O_{g_d}(z_d,t)}{\partial z_d} + D_{gd}\frac{\partial^2 O_{g_d}(z_d,t)}{\partial z_d^2} - \frac{(1-\varepsilon_{gd})}{\varepsilon_{gd}} K_{la}\left(\frac{O_{gd}(z_d,t)}{H} - O_{ld}(z_d,t)\right) \quad \ldots(3)$$

For liquid phase oxygen concentration in the downcomer:

$$\frac{\partial O_{l_d}(z_d,t)}{\partial t} = -v_{gd}\frac{\partial O_{l_d}(z_d,t)}{\partial z_d} + D_{gd}\frac{\partial^2 O_{l_d}(z_d,t)}{\partial z_d^2} + K_{la}\left(\frac{O_{gd}(z_d,t)}{H} - O_{ld}(z_d,t)\right) \quad \ldots(4)$$

Where

H: is the Henry's law constant.

3.3. Gas separator section

For the gas oxygen concentration:

$$\frac{\partial O_{gt}}{\partial t} = \frac{\varepsilon_{gr}A_r v_{gr}O_{gr}(z_r=L_r) - \varepsilon_{gd}A_d v_{gd}O_{gd}(z_d=0) - Q_{g,out}O_{gt}}{\varepsilon_{gt}V_t} - \left(\frac{1-\varepsilon_{gt}}{\varepsilon_{gt}}\right)K_{la}\left(\frac{O_{gt}}{H} - O_{lt}\right) \quad \ldots(5)$$

For the liquid oxygen concentration:

$$\frac{\partial O_{lt}}{\partial t} = \frac{(1-\varepsilon_{gr})A_r v_{lr}O_{lr}(z_r=L_r) - (1-\varepsilon_{gd})A_d v_{ld}O_{ld}(z_d=0)}{(1-\varepsilon_{gt})V_t} + K_{la}\left(\frac{O_{gt}}{H} - O_{lt}\right) \quad \ldots(6)$$

Table 1 lists the initial and boundary conditions which are used to solve these equations.

Table 1,
Initial and Boundary Conditions for Each Section of the Present ALR .

Riser section	I.C.	Gas	$O_{gr}(0 \le z_r \le L_r, t=0)=0$
	B.C.1		$O_{gr}(z_r=0, t>0) = \left(\frac{v_{gd}A_d O_{gd}(z_r=0,t>0)+Q_{g,in}O_{g,in}}{v_{gr}A_r}\right)$
	B.C.2		$Q_{g,in} = inlet\ gas\ \ flowrate\ (\mathrm{m}^3/\mathrm{s})$ $O_{gr}(z_r=L_r, t>0)=O_{gt}(t>0)$
	I.C.	Liquid	$O_{lr}(0 \le z_r \le L_r, t=0)=0$
	B.C.1		$O_{lr}(z_r=0, t>0)=O_{ld}(z_d=L_d, t>0)$
	B.C.2		$O_{lr}(z_r=L_r, t>0)=O_{lt}(t>0)$
Downcomer section	I.C.	Gas	$O_{gd}(0 \le z_d \le L_d, t=0)=0$
	B.C.		$O_{gd}(z_d=0, t>0)=O_{gt}(t>0)$
	I.C.	Liquid	$O_{ld}(0 \le z_d \le L_d, t=0)=0$
	B.C.		$O_{ld}(z_d=0, t>0)=O_{lt}(t>0)$
Gas Separator section	I.C.	Gas	$O_{gt}(t=0)=0$
		Liquid	$O_{lt}(t=0)=0$

I.C.: Initial Condition B.C.: Boundary Condition

4. Hydrodynamic and Gas-Liquid Mass Transfer Correlations

Hydrodynamic behavior is essential for the understanding of the phenomena taking place in ALR. Due to their strong influence on mass transfer performance, they have received considerable attention from most investigators. Hydrodynamic parameters of interest in design are the overall gas holdup, the gas holdups in the riser and in the downcomer, the magnitude of the induced liquid circulation and the liquid phase dispersion coefficients in various regions of the reactor.

4.1. Gas Holdup Correlations

The volume fraction of gas (or gas holdup) is an essential parameter for the design of airlift contactors. Due to the configuration of airlift contactors that allow aeration in the riser, gas holdup in riser is usually higher than the downcomer. This difference in gas holdups is the main cause of pressure difference, which creates liquid circulation pattern.

The overall gas holdup in term of riser, downcomer and gas separator gas holdups was calculated using the following equation (Chisti, 1989; Zhonghuo, 2010):

$$\varepsilon_{gr} = \varepsilon_g + (A_d / A_r)(\varepsilon_g - \varepsilon_{gd}) \quad \ldots(7)$$

Where
ε_g : is overall gas holdup
ε_{gr} : is the riser gas holdup
ε_{gd} : is the downcomer gas holdup

4.2. Gas-Liquid Mass Transfer Correlations

The rate of mass transfer from gas to liquid phase may be expressed in terms of an overall volumetric mass transfer coefficient, $K_l a$ based on gas liquid dispersion volume. This coefficient is also an important indicator for comparing the oxygen transfer capabilities of various aerobic bioreactors. The volumetric oxygen transfer coefficient is defined by the following equation (Zhonghuo et al., 2010; Chisti and Young, 1987):

$$K_l a = n_{O_2} / \Delta C \quad \ldots(8)$$

Where n_{O_2} is the flux of oxygen transfer between phases, ΔC the concentration driving force between the phases.

The gas-liquid interfacial area based on liquid volume or gas-liquid dispersion volume (a_l or a_D, respectively) need to be determined to evaluate

overall mass transfer coefficient ($K_l a$). The value of a_l and a_D can be evaluated from Eq. (9) and Eq. (10), respectively (Chisti, 1998):

$$a_l = 6\varepsilon_g /[d_B(1-\varepsilon_g)] \quad \ldots(9)$$

$$a_D = 6\varepsilon_g / d_B \quad \ldots(10)$$

However, instead of determining K_l and a separately, the mass transfer behavior in these systems are usually presented in terms of the overall mass transfer coefficient ($K_l a$) which was often determined using empirical correlations reported in literature.

4.3. Liquid velocity

The liquid circulation in airlift reactors originates from the difference in the bulk densities of the fluids in the riser and the downcomer. The liquid circulates a well defined path: up flow in the riser, downflow in the downcomer. The predicted superficial liquid velocities in the airlift reactor were calculated using the following well known tested equation developed by Chisti, (1989):

$$U_{lr} = \left[\frac{2gh_D(\varepsilon_{gr}-\varepsilon_{gd})}{K_B(A_r/A_d)^2(1/(1-\varepsilon_{gd})^2)}\right]^{0.5} \quad \ldots(11)$$

Where

$$K_B = 11.40\left(\frac{A_d}{A_b}\right)^{0.79} \quad \ldots(12)$$

The height of the dispersion h_D was calculated from the following known equation:

$$h_D = \frac{h_l}{1-\varepsilon_g} \quad \ldots(13)$$

The linear liquid velocity in the riser and downcomer can be calculated from the superficial liquid velocity as follows (Chisti, 1989):

$$v_{lr} = \frac{U_{lr}}{1-\varepsilon_{gr}} \quad \ldots(14)$$

$$v_{lr}(1-\varepsilon_{gr})A_r = v_{ld}(1-\varepsilon_{gd})A_d \quad \ldots(15)$$

5. Solving the mathematical model

The mathematical model provides a set of differential equations for oxygen concentration in the riser, downcomer and gas separator. These equations to be solved simulated simultaneously using FINITE ELEMENTS technique in MATLAB V-2008A software package.

Figure (2) represent the algorithm for the computer simulation which is used to simulate oxygen concentration for a given reactor geometry and gas flow.

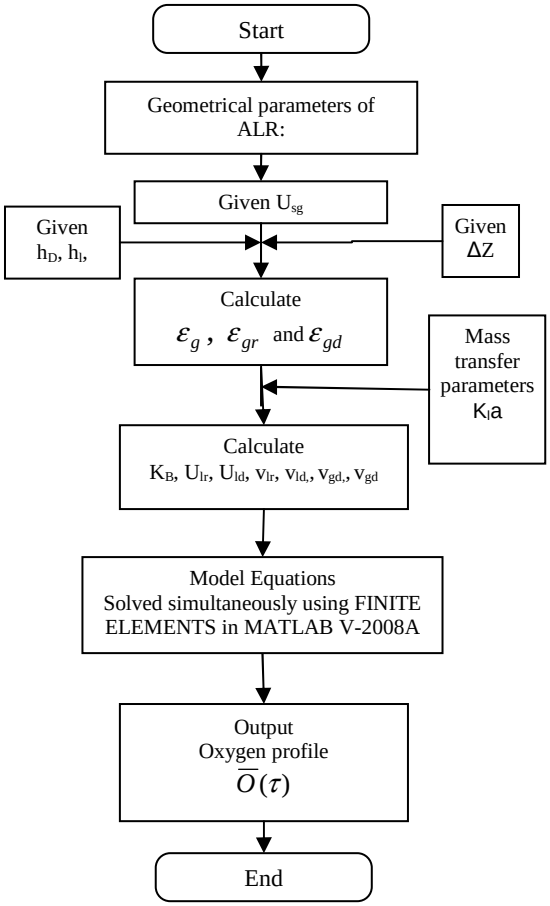

Fig. 2, Algorithm for the Computer Simulation Procedure to Simulate Oxygen Concentration for the Present ALR Geometry and Gas Flow .

6. Experimental Work

6.1. Airlift Reactor

The proposed airlift reactor consists of two concentric-tubes with dimensions given in Table 2. The volume of the reactor was 45 liter and A_d/A_r=4.29. The water level in the reactor was 1.1 cm. The tubes were constructed of transparent poly acyclic with the bottom and top plates made of rigid nylon. Water manometer was used to measure the pressure drop across the reactor and the distance between the two manometer reading

points was 100 cm. Air spargers and other pipes were constructed of copper. Figure (3) shows the schematic arrangement of the experimental apparatus.

Table 2,
Dimensions of a Concentric Tube Airlift Reactor .

	Height (cm)	Diameter (D_o) (cm)	Diameter (D_i) (cm)
Main column	150	23.6	23.0
Draft tube	1.00	10.6	10.0

Air was sparged through 8 cm diameter circular sparger, with 24 holes of 1 mm diameter. Air flow rates were measured by a two type's rotameters (Rota Company of QVF type). The first one is used for the low flow rates (max. reading 1 m^3/h) and the second one for the higher rate (max. reading 10 m^3/h). All experimental runs were carried out at atmospheric pressure and a temperature of 29˚C. A series of experiments were performed by varying the superficial gas velocity (with respect to the cross-sectional area of the riser) over the range of 0.01–0.164 ms^{-1} to create a characteristic velocity curve of the airlift reactor.

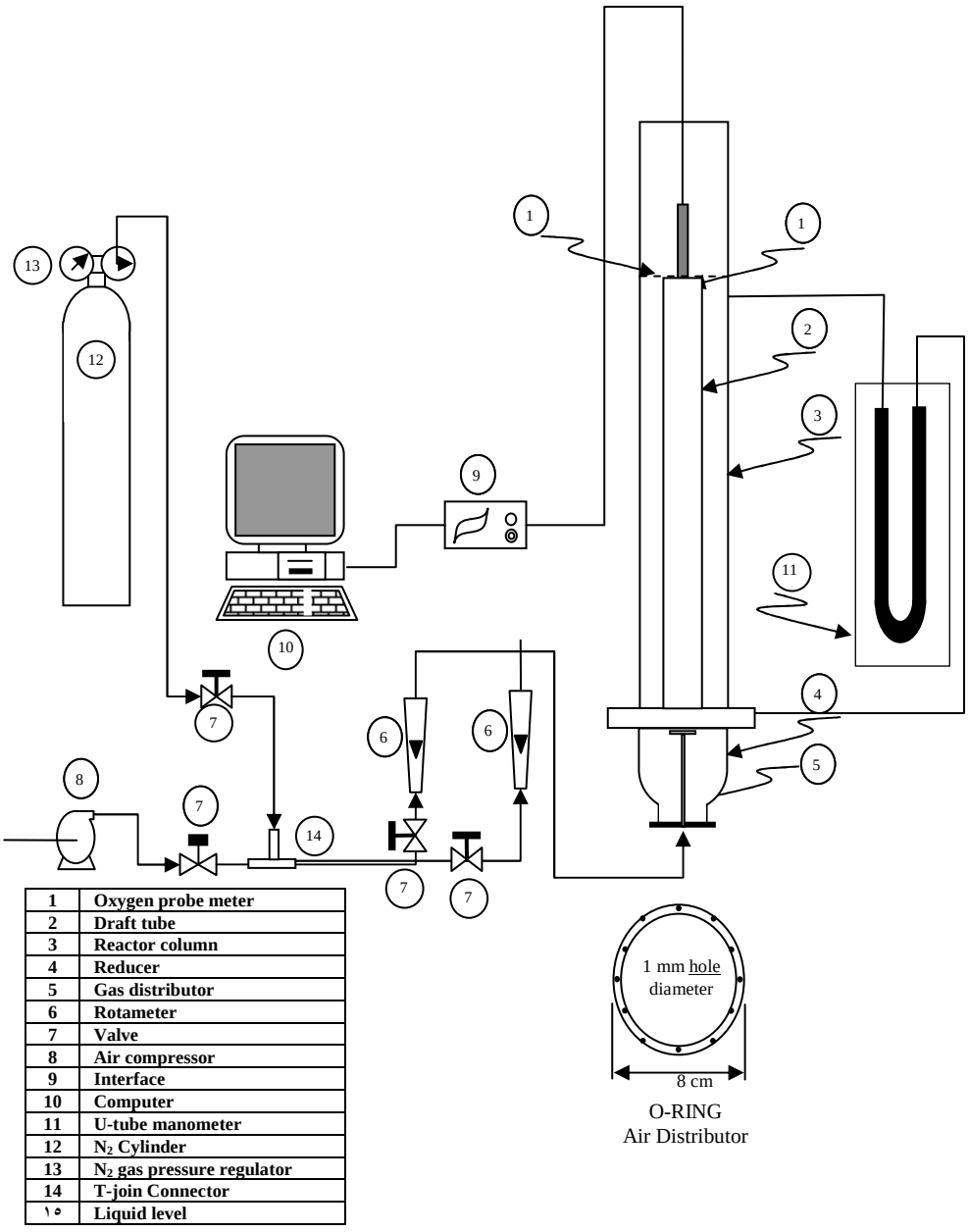

1	Oxygen probe meter
2	Draft tube
3	Reactor column
4	Reducer
5	Gas distributor
6	Rotameter
7	Valve
8	Air compressor
9	Interface
10	Computer
11	U-tube manometer
12	N_2 Cylinder
13	N_2 gas pressure regulator
14	T-join Connector
١٥	Liquid level

Fig.3.Experimental Setup of ALR.

6.2. Measurement of volumetric mass transfer coefficient

The overall volumetric mass transfer coefficient, $K_l a$, was determined by the dynamic gassing method (Bouaifi et al., 2001; Chisti, 1989). The dissolved oxygen concentration in the batch liquid phase was measured by means of an oxygen probe inserted horizontally at 0.1 m below the exit of the riser that was connected to a dissolved oxygen-meter type Lutron DO-5510. The oxygen probe signals were measured using A/D converter and recorder on a PC. In each experimental run, tap water has been first stripped of oxygen by the dynamic gassing method by bubbling N_2 gas through the gas sparger. This step will continue till the probe reading becomes zero. After that the nitrogen gas flow was turned off and the flow switched to the air flow with a specific volumetric flow rate using the rotameter then the dissolved oxygen concentration was recorded with respect to time as air is distributed into the ALR and until the water became saturated with oxygen.

7. Method of Calculations

7.1. Gas hold-up

The total gas holdup was determined by the expansion volume method (Chisti, 1989).
This method was chosen because it was the simplest to use. The gas holdup was estimated as the percentage increase in volume of the gassed liquid compared with ungassed liquid volume. In this airlift bioreactor the variation of liquid volume can be determined by observing the height of the surface of the ungassed liquid and aerated liquid. The dispersion height was estimated by observing the position of the liquid level on a graduated stainless-steel rod suspended from the vessel top plate. At high gas flow rates the liquid surface become very turbulent, with the level changing erratically, and so a mean dispersion height was estimated (Chisti, 1989).
Because the volume of gas cannot be measured directly, we defined V_D (dispersed volume) as the total volume of gas phase plus volume of liquid phase. Then

$$\varepsilon_g = \frac{V_D - V_l}{V_D} \qquad \ldots(16)$$

$$\varepsilon_g = 1 - \frac{h_l A}{h_D A} \qquad \ldots(17)$$

Finally, $\varepsilon_g = 1 - \frac{h_l}{h_D}$ …(18)

Where:
h_D dispersed liquid height (cm) and h_l liquid height (cm).

The downcomer gas holdup was estimated by measuring the pressure difference between the two measuring ports of the column and by using the following equation (Chisti, 1989):

$$\varepsilon_{gd} = 1 - \frac{\Delta Z_{manometer}}{\Delta H} \qquad \ldots(19)$$

Where:
ΔZ: distance of liquid level in manometer,
ΔH: distance of liquid level.

7.2. Mass transfer coefficient

The $K_l a$ is determined as mentioned in the previous section by using the dynamic method. The investigations of mass transfer characteristics were restricted to oxygen transfer only, and in all investigations, the ALR systems were subject to the following assumptions (Wongsuchoto, 2002):

- Gas composition is constant.
- The system is isothermal, and the effect of the dynamics of the dissolved oxygen electrode is negligible.
- For sparingly soluble gases such as oxygen, the liquid phase volumetric mass transfer coefficient ($k_l a$) is nearly equal in value to that of the overall volumetric mass transfer coefficient ($K_l a$).

A material balance on dissolved oxygen according to the above assumption gives the following equation (Wongsuchoto, 2002):

$$\frac{dO}{dt} = k_l a(O^* - O) = K_l a(O^* - O) \qquad \ldots(20)$$

O^*: saturation dissolved oxygen concentration.
O: dissolved oxygen concentration in liquid phases.
Integrate Eq. (6) with the limits of $O = O_0$ at $t = 0$ and $O = O$ at $t = t$ results in:

$$\int_{O_\circ}^{O} \frac{dO}{(O^* - O)} = K_l a \int_0^t dt \qquad \ldots(21)$$

The result of integration is

$$\ln\left[\frac{(O^* - O_\circ)}{(O^* - O)}\right] = K_l a t \qquad \ldots(22)$$

The value of $K_l a$ is obtained from the slope of the linear regression with

$\ln\left[\frac{(O^* - O_\circ)}{(O^* - O)}\right]$ with respect to time (t).

8. Results and Discussion

8.1. Effect of Superficial Gas Velocity on Gas Holdups

The effect of superficial gas velocity on the overall, riser and downcomer gas holdups can be represented in Fig. 4. As the superficial gas velocity increases the gas holdups increases. Generally, the experimental gas holdup profiles are linear with respect to u_{sg} for the overall, riser, and downcomer gas holdups. This means that the slip of relative velocity between the gas and liquid phases does not change with increased gas through put.

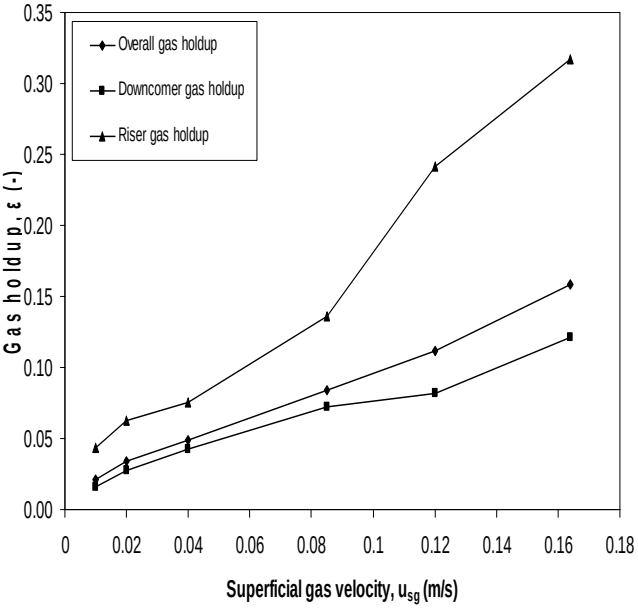

Fig. 4. Relationship Between Overall, Riser and Downcomer Gas Holdups and Superficial Gas Velocity of the Present ALR.

The experimental data have been simulated with the following equation (Chisti, 1989):

$$\varepsilon_{gi} = \lambda u_{sg}^{\gamma} \quad \ldots(23)$$

Where λ and γ are constants, and the final result for overall, and dowcomer holdups can be expressed as:

$$\varepsilon_g = 0.643 u_{sg}^{0.799} \quad \ldots(24)$$

$$\varepsilon_{gd} = 0.428 u_{sg}^{0.728} \quad \ldots(25)$$

The values of riser gas holdup were estimated using Eqn. (7).

The simulated gas fraction over predicted empirical data, are compared as shown in Fig. 5. It can be concluded that the profile also has a linear form with acceptable accuracy.

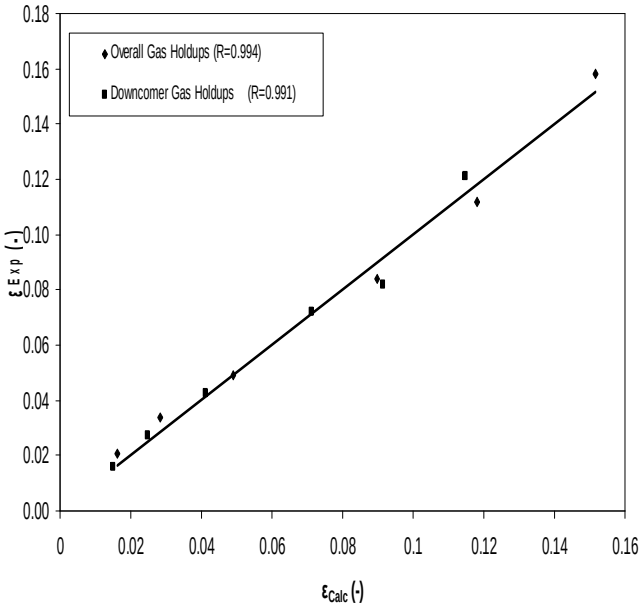

Fig.5. Comparison between Experimental and Predicted Overall and Downcomer Gas Holdups at the Same Superficial Gas Velocity of the Present ALR .

8.2. Effect of Superficial Gas Velocity on Internal Liquid Circulation

Liquid velocity in airlift reactors affects the mixing characteristics of fluids, i.e. volumetric mass transfer coefficient, which determines the performance of the reactor. Figure (6) shows the experimental results of the effect of u_{sg} on linear liquid velocity in the riser and downcomer. It can be observed that an increase in gas velocity effectively implied a large energy input to the system and high liquid velocity was induced both in riser and downcomer. The riser and downcomer liquid velocities were determined from eqn. (14) and the mass conservation equation (15) including the effect of both riser and downcomer gas holdups. All configurations demonstrated the less values of downcomer liquid velocity than riser liquid velocity. It was because, in the present experiment work, the cross sectional of the downcomer area was 4.29 times larger than that of

the riser. Hence, all downcomer liquid velocities were lower than riser liquid velocities based on the continuity equation.

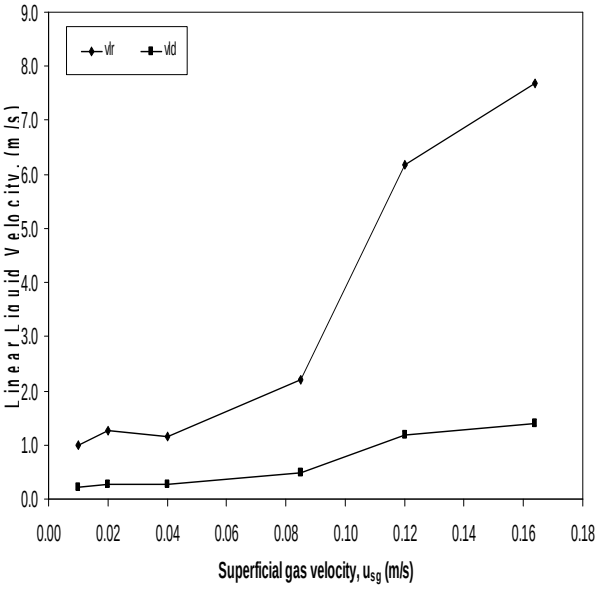

Fig. 6. Relationship Between Linear Liquid Riser and Downcomer Velocities and Superficial Gas Velocity for the Present ALR.

8.3. Effect of Superficial Gas Velocity on the Overall Oxygen Mass Transfer Coefficient

Figure 7 shows the normalized oxygen concentration-time experimental data. These data were processed with eqn. (22) and the final results were presented by Fig. (8).

The value of $K_l a$ is obtained from the slope of the linear regression with $\ln\left[\frac{(O^* - O_\circ)}{(O^* - O)}\right]$ with respect to dimensionless time (τ). The obtained $K_l a$ values where also plotted versus u_{sg} and the relationship between them is illustrated in Fig. 9. It can be shown from Fig. 9 that the value of $K_l a$ increases with increasing u_{sg}. The smallest quantity of air means the lowest liquid velocity, and the low liquid velocity means that there was a rather low level of gas bubbles in the reactor which reduce the interfacial area of gas for mass transfer in the system. At high gas velocity, the liquid velocity increases which in turn generate finer bubbles, and thus increased gas holdup. The higher gas holdup results in higher interfacial area which increases $K_l a$.

An attempt has been made to correlate the obtained $K_l a$ values with the following equation (Chisti, 1989):

$$K_l a = \alpha u_{sg}^{\beta} \quad \ldots(25)$$

The following empirical equation, best relating the volumetric mass transfer coefficient with the superficial gas velocity:

$$K_l a = 0.229 u_{sg}^{0.738} \quad \ldots(26)$$

Equation (26) was obtained by multiple regression analysis with a correlation coefficient of 0.997. Figure 10 shows a comparison between experimental and predicted values of $K_l a$. It can be seen that the correlation satisfies the experimental data of the present system.

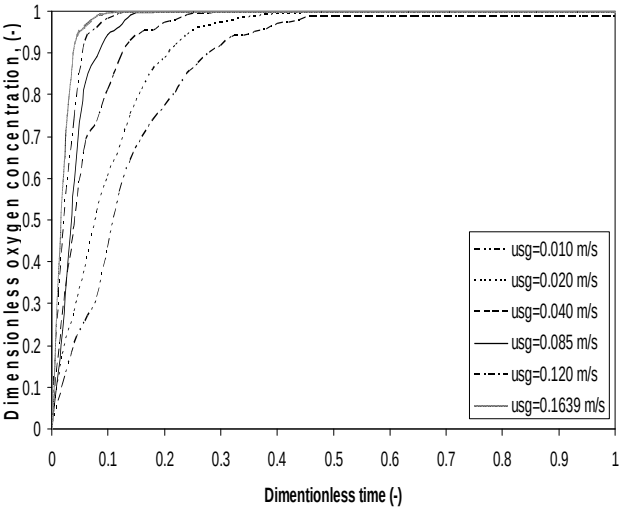

Fig. 7. Relationship between Dimensionless Oxygen Concentration and Dimensionless Time at Different Superficial Gas Velocity for the Present ALR .

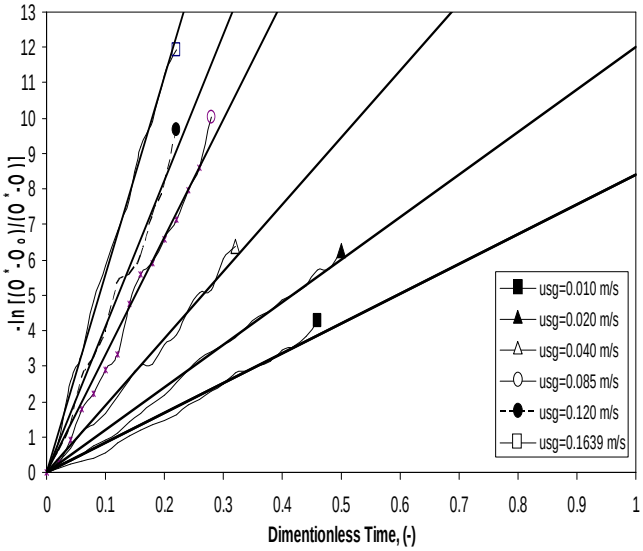

Fig.8. Logarithmic Oxygen Concentration vs. Dimensionless Time of the Mathematical Model at Various u_{sg} Values .

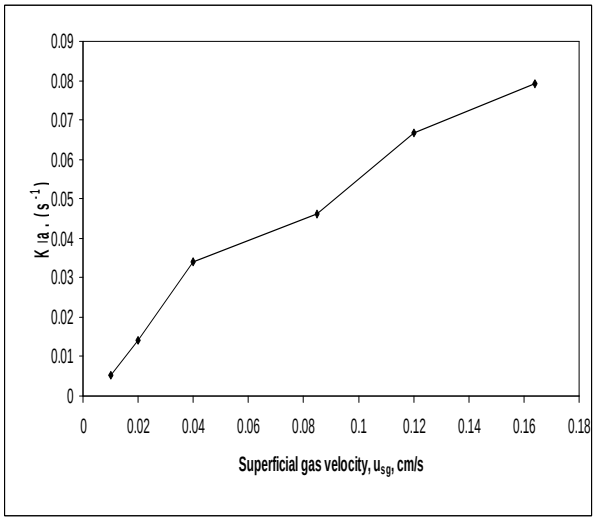

Fig. 9. Relationship between Overall Volumetric Oxygen Mass Transfer Coefficient and Superficial Gas Velocity for the Present ALR.

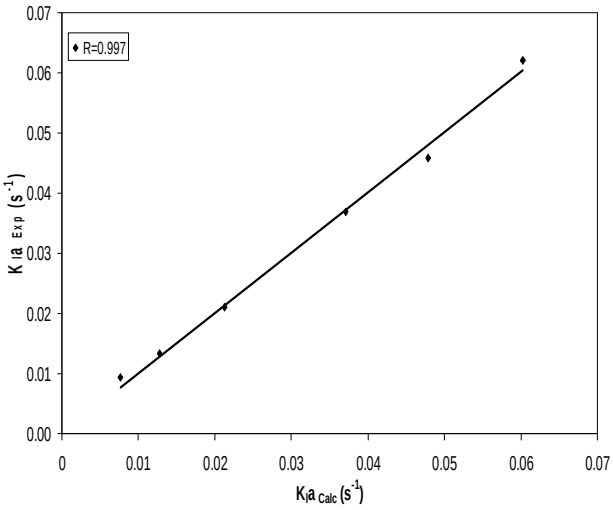

Fig. 10. Comparison Between Experimental and Predicted Overall Volumetric Oxygen Mass Transfer Coefficient at the Same and Superficial Gas Velocity of the Present ALR .

8.4. Mathematical Model Parameters Determination

In order to simplify the solution of the mathematical model differential equations. Equation (1) to (6) can be converted into a dimensionless form by introducing the following dimensionless variables and using the initial and boundary conditions in Table 2:

$$\tau = \frac{t}{T} = \frac{t v_{ld} A_d}{V_r} \quad \ldots(28)$$

$$Z = \frac{z}{L} \quad \ldots(29)$$

$$\overline{O}_L = \frac{O_L}{O_L^*} \quad \ldots(30)$$

$$\overline{O}_g = \frac{O_g}{O_{g,in}^*} \quad \ldots(31)$$

Riser section

For gas phase oxygen concentration:

$$\frac{\partial \overline{O}_{g\,r}}{\partial \tau_r} = -\frac{v_{gr} T}{L_r}\frac{\partial \overline{O}_{g\,r}}{\partial z_r} + \frac{D_{gr} T}{L_r^2}\frac{\partial^2 \overline{O}_{g\,r}}{\partial z_r^2} - \frac{(1-\varepsilon_{gr}) K_{La} T}{\varepsilon_{gr}}\left[\overline{O}_{gr}(Z_r) - \overline{O}_{lr}(Z_r)\right] \quad \ldots(32)$$

For liquid phase oxygen concentration:

$$\frac{\partial \overline{O}_{l\,r}}{\partial \tau_r} = -\frac{v_{lr} T}{L_r}\frac{\partial \overline{O}_{l\,r}}{\partial z_r} + \frac{D_{lr} T}{L_r^2}\frac{\partial^2 \overline{O}_{l\,r}}{\partial z_r^2} - K_{la} T\left[\overline{O}_{gr}(Z_r) - \overline{O}_{lr}(Z_r)\right] \quad \ldots(33)$$

Downcomer section

For gas phase oxygen concentration:

$$\frac{\partial \overline{O}_{g\,d}}{\partial \tau_d} = -\frac{v_{gd} T}{L_d}\frac{\partial \overline{O}_{g\,d}}{\partial z_d} + \frac{D_{gd} T}{L_d^2}\frac{\partial^2 \overline{O}_{g\,d}}{\partial z_d^2} - \frac{(1-\varepsilon_{gd}) K_{la} T}{\varepsilon_{gd}}\left[\overline{O}_{gd}(Z_d) - \overline{O}_{ld}(Z_d)\right] \quad \ldots(34)$$

For liquid phase oxygen concentration in the downcomer:

$$\frac{\partial \overline{O}_{l\,d}}{\partial \tau_d} = -\frac{v_{ld} T}{L_d}\frac{\partial \overline{O}_{l\,d}}{\partial z_d} + \frac{D_{ld} T}{L_d^2}\frac{\partial^2 \overline{O}_{l\,d}}{\partial z_d^2} - K_{la} T\left[\overline{O}_{gd}(Z_d) - \overline{O}_{ld}(Z_d)\right] \quad \ldots(35)$$

Gas separator section

For the gas oxygen concentration:

$$\frac{\partial \overline{O}_{gt}}{\partial \tau_t} = \frac{TQ_{gr}}{\varepsilon_{gt} V_t}\overline{O}_{gr}(Z_r = L_r) - \frac{TQ_{g,out}}{\varepsilon_{gt} V_t}\overline{O}_{gt} - \frac{TQ_{gd}}{\varepsilon_{gt} V_t}\overline{O}_{gt} - \left(\frac{1-\varepsilon_{gt}}{\varepsilon_{gt}}\right) K_{la} T\left(\overline{O}_{gt} - \overline{O}_{lt}\right) \quad \ldots(36)$$

For the liquid oxygen concentration:

$$\frac{\partial \overline{O}_{lt}}{\partial \tau_t} = \frac{TQ_{Lr}}{(1-\varepsilon_{gt}) V_t}\overline{O}_{lr}(Z_r = L_r) - \frac{TQ_{l,out}}{(1-\varepsilon_{gt}) V_t}\overline{O}_{lt} - \frac{TQ_{ld}}{(1-\varepsilon_{gt}) V_t}\overline{O}_{lt} - K_{la} T\left(\overline{O}_{gt} - \overline{O}_{lt}\right) \quad \ldots(37)$$

Table 3,
Initial and Boundary Conditions in Dimensionless Form .

Riser section	I.C.	Gas	$\overline{O}_{gr}\left(0 \le Z_r \le 1, \tau = 0\right) = 0$
	B.C.1		$\overline{O}_{gr}\left(Z_r = 0, \tau > 0\right) = \left(\frac{v_{gd} A_d \overline{O}_{gd}\left(Z_r = 0, \tau > 0\right) + Q_{g,in} \overline{O}_{g,in}}{v_{gr} A_r} \right)$
	B.C.2		$Q_{g,in} = inlet\ gas\ \ flowrate\ (\mathrm{m}^3/\mathrm{s})$ $\overline{O}_{gr}\left(Z_r = 1, \tau > 0\right) = \overline{O}_{gt}\left(\tau > 0\right)$
	I.C.	Liquid	$\overline{O}_{lr}\left(0 \le Z_r \le 1, \tau = 0\right) = 0$
	B.C.1		$\overline{O}_{lr}\left(Z_r = 0, \tau > 0\right) = \overline{O}_{ld}\left(Z_d = 1, \tau > 0\right)$
	B.C.2		$\overline{O}_{lr}\left(Z_r = 1, \tau > 0\right) = \overline{O}_{lr}\left(\tau > 0\right)$
Downcomer section	I.C.	Gas	$\overline{O}_{gd}\left(0 \le Z_d \le 1, \tau = 0\right) = 0$
	B.C.		$\overline{O}_{gd}\left(Z_d = 0, \tau > 0\right) = \overline{O}_{gt}\left(\tau > 0\right)$
	I.C.	Liquid	$\overline{O}_{ld}\left(0 \le Z_d \le 1, \tau = 0\right) = 0$
	B.C.		$\overline{O}_{ld}\left(Z_d = 0, \tau > 0\right) = \overline{O}_{lt}\left(\tau > 0\right)$
Gas Separator section	I.C.	Gas	$\overline{O}_{gt}\left(\tau = 0\right) = 0$
		Liquid	$\overline{O}_{lt}\left(\tau = 0\right) = 0$

I.C. : Initial Condition B.C.: Boundary Condition.

The proposed mathematical model supplies a set of partial differential equations for oxygen transfer. The solution of these equations was solved simultaneously with the geometric, mass transfer and hydrodynamic parameters using FINITE ELEMENTS in MATLAB V-2008A software package.

The oxygen concentration in liquid phase of the present internal loop airlift reactor was predicted by dispersion model. To predict oxygen concentration in liquid phase, hydrodynamic and mass transfer parameters including gas holdups (ε_g), liquid velocities (v_l), gas velocities (v_g), dispersion coefficients (D), geometrical parameters and overall volumetric gas-liquid mass transfer coefficient ($K_l a$) had to be known in a prior. Table 4 employed the correlations used in the present mathematical model.

Table 4,
Empirical Hydrodynamic Correlations used in the Mathematical Model.

Correlations	
$\varepsilon_g = 0.643 u_{sg}^{0.799}$	…(24)
$\varepsilon_{gd} = 0.428 u_{sg}^{0.728}$	…(25)
$K_l a = 0.229 u_{sg}^{0.738}$	…(26)
assuming that $\varepsilon_{gt} = \varepsilon_{gr}$	

Other parameters such as the downcomer liquid velocity (v_{ld}) were calculated from eqn. (14), while the riser liquid velocity was calculated from the continuity eqn. (15).

Riser gas velocity v_{gr} was calculated from v_{lr} and slip velocity in the riser v_{sr} as follows (Chisti, 1989):

$$v_{gr} = v_{lr} + v_{sr} \qquad \ldots(37)$$

v_{sr} did not vary much with conditions in the ALR, and it was assumed here to be constant at 0.25 m/s as it reported by Chisti, (1989). Downcomer gas velocity v_{gd} was calculated, in a similar fashion, using the continuity equation (Chisti, 1989):

$$v_{gd} = \frac{v_{gr} A_r \varepsilon_{gr} - Q_{g,in}}{A_d \varepsilon_{gd}} \qquad \ldots(38)$$

D_{gr}, D_{gd}, D_{lr} and D_{ld} as dispersion coefficients in the gas and liquid phases for both the riser and downcomer remained unknown. The liquid phase dispersion coefficients values, D_{lr} *and* D_{ld} were reported by several investigators and employed in this model directly without manipulation (Chisti, 1989, Kochbeck and Hempel, 1994; Merchuk et al., 1998). Also, Gas phase dispersion coefficients (D_{gr} and D_{gd}) were reported by Chisti, (1989) to

be 2 - 5 m^2/s for the ALR at u_{sg} between 0.01-0.1 m/s.

In order to verify the sensitivity of the simulation results with the variation of the dispersion coefficients for liquid and gas phases. Preliminary simulations were conducted and it was found that the time-oxygen concentration profiles from the various simulations of different values of dispersion coefficients in the range reported in the previous paragraph were not significantly different from each other. This indicated that, within the range of dispersion coefficients reported in literature, there was no meaningful difference in the responding time to reach equilibrium concentration. Hence, the values of D_{lr}, D_{ld}, D_{gr}, D_{gd} used in all simulations were selected arbitrarily as 0.01, 0.01, 2 and 2 m^2/s, respectively.

To verify the ability of the model in predicting oxygen mass transfer behavior between gas and liquid phases in the internal loop ALR, the simulation results were compared with experimental data. Figure 11 illustrates the comparisons between the simulation results and experimental data on liquid phase oxygen concentration in the riser (O_{lr}) in the system at different superficial gas velocities (u_{sg}). In general, both simulation results and experimental data demonstrated that the oxygen concentration profile reached equilibrium concentration more rapidly with increasing u_{sg}. It can be concluded that the predicted model results give a reasonable accuracy when compared with experimental data for the same range of u_{sg}.

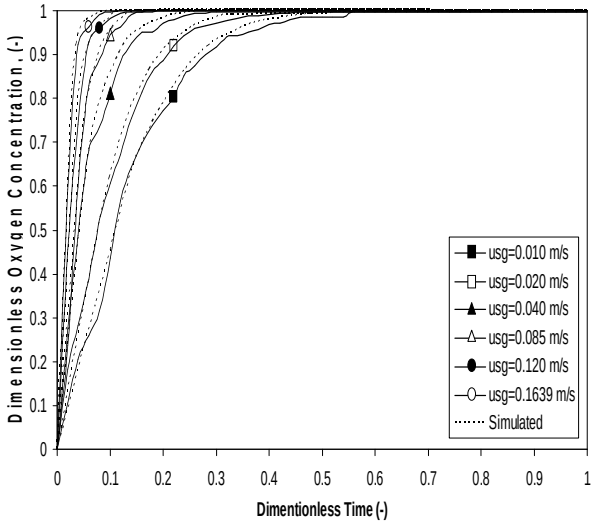

Fig. 11. Comparison Between Experimental and Simulated Data of Oxygen-Time Profiles in the Riser Region of the Present ALR .

List of Abbreviations, Notations and Greek Letters

Abbreviations

ALR	Airlift reactor	
A	cross-sectional area	m^2
a	Specific gas-liquid interfacial area of bubble per volume of reactor	$m^2\ m^{-3}$
A_b	Cross sectional area for flow under baffle or draft tube	m^2
O	Instantaneous oxygen concentration in the liquid	kgm^{-3}
O^*	Saturation dissolved oxygen concentration in the liquid	kgm^{-3}
O_o	Initial oxygen concentration in the liquid	kgm^{-3}
D	Dispersed phase	-
D_g	Gas phase dispersion coefficient	M^2s^{-1}
d_B	Bubble diameter	m
g	Gravitational acceleration	ms^{-2}
H	Henery's Law constant	-
H_D	Dispersion height	m
H_L	Unaerated liquid height	m
K_la	Overall mass transfer coefficient	s^{-1}
L	Length	m
L_b	bottom clearance	m
n	Moles of a oxygen gas	mol
O_g	Oxygen concentration in gas phase	kgm^{-3}
O_{gd}	Oxygen concentration in gas phase of the downcomer section	kgm^{-3}
O_{gr}	Oxygen concentration in gas phase of the riser section	kgm^{-3}
O_l	Oxygen concentration in liquid phase	kgm^{-3}
O_{ld}	Oxygen concentration in liquid phase of the downcomer section	kgm^{-3}
O_{lr}	Oxygen concentration in liquid phase of the riser section	kgm^{-3}
T	Time	s
T	Time	s
u_{sg}	Superficial gas velocity	ms^{-1}
U_L	Superficial liquid velocity	ms^{-1}
V	Volume	m^3
v_G	Linear gas velocity	ms^{-1}
v_L	Linear liquid velocity	ms^{-1}
v_s	Slip velocity	ms^{-1}
Z	Dimensionless length	-

Greek letter

ΔC	Concentration driving force between the two phases	kgm^{-3}
ΔH	Distance of liquid level	m
ΔZ	Distance of liquid level in a manometer	m
ε_g	Gas holdup	-
ε_{go}	Overall gas holdup	-
ε_{gd}	Gas holdup in the downcomer section	-
ε_{gr}	Gas holdup in the riser section	-
τ	Dimensionless time	-
α	Constant	
β	Constant	
γ	Constant	
λ	Constant	

9. Conclusions

In the present study, oxygen mass transfer could be well described by the proposed mathematical model based on a set of continuity equations. The obtained empirical equations for the gas holdups, overall oxygen mass transfer coefficient gave good results and high accuracy for the present ALR. The simulated results based on the obtained empirical equations, the dispersion model for the riser and downcomer and the perfect mixed model for the gas-liquid separator, agreed well with the experimental results over the studied range of operating conditions.

10. Acknowledgement

This study was supported by a grand provided by the Ministry of Higher Education and Scientific Research/ Research and Development Department. Authors gratefully acknowledge this contribution and supporting.

11. References

[1] André, G., Robinson, C.W., and Young, M.M., (1983), "New criteria for application of the well-mixed model to gas-liquid mass transfer studies", Chem. Eng. Sci., 38: 1845-1984.

[2] Bouaifi, M., Hebrard, G., Bastoul, D., and Roustan, M., (2001), "A comparative study of gas hold-up, bubble size, interfacial area and mass transfer coefficients in stirred gas-liquid reactors and bubble columns", Chem. Eng. Proc., 97-111.

[3] Camarasa E., L.A.C. Meleiro, E. Carvalho, A. Domingues, R. Maciel Filho, G. Wild, S. Poncin, N. Midoux, and J. Bouillard, (2001), "A complete model for oxidation air-lift reactors", Computers and Chemical Engineering, 25, 577–584.

[4] Cerri M.O., A.C. Badino, (2010), "Oxygen transfer in three scales of concentric tube airlift bioreactors", Biochemical Engineering Journal, 51, 40–47.

[5] Chisti Y., (1989), "Airlift Bioreactors", Elsevier Applied Science, London.

[6] Chisti, M.Y., (1998), "Pneumatically agitated bioreactors in industrial and environmental bioprocessing: hydrodynamics", Appl. Mech. Rev. 51: 33-112.

[7] Chisti, M.Y., and Young, M.M., (1987), "Airlift reactors: characteristics, applications and design considerations", Chem. Eng. Commun., 60: 195-242.

[8] Dhaouadi, H., Poncin, S., Midoux, N., and Wild, G., (2001), "Gas-liquid mass transfer in an airlift reactor—analytical solution and experimental confirmation", Chem. Eng. Proc., 40: 129-133.

[9] Fields, P.R., and Slater, N.K.H., (1983), "Tracer dispersion in a laboratory air-lift reactor", Chem. Eng. Sci., 38: 647-653.

[10] Giovannettonea J.P., E. Tsaib, J.S. Gulliver, (2009),"Gas void ratio and bubble diameter inside a deep airlift reactor", Chemical Engineering Journal, 149, 301–310.

[11] Guillermo Quijano, Sergio Revah, Mariano Gutierrez-Rojas, Luis B. Flores-Cotera and Frederic Thalasso, (2009), "Oxygen transfer in three-phase airlift and stirred tank reactors using silicone oil as transfer vector", Process Biochemistry, 44, 619–624.

[12] Koch beck, B., and Hempel, D.C., (1994), "Liquid velocity and dispersion coefficient in an airlift reactor with inverse internal loop", Chem. Eng. Technol., 17: 401- 405.

[13] Merchuk, J.C., and Yunger, R., (1990), "The role of the gas-liquid separator of airlift reactors in the mixing process", Chem. Eng. Sci., 45: 2973-2975.

[14] Merchuk, J.C., Contreras, A., Garcia, F., and Molina, E., (1998), "Studies of mixing in a concentric tube airlift bioreactor with

different spargers", Chem. Eng. Sci. 53: 709-719.

[15] Peter M. Kilonzo, Argyrios Margaritis, and M.A. Bergougnou, (2010), "Hydrodynamic characteristics in an inverse internal-loop airlift-driven fibrous-bed bioreactor", Chemical Engineering Science, 65, 692–707.

[16] Tongwang Zhang, Tiefeng Wang and Jinfu Wang, (2005), "Mathematical modeling of the residence time distribution in loop reactors", Chemical Engineering and Processing, 44, 1221–1227.

[17] Verlaan, P., van Eija, A.M.M., Tramper, J., and van't Riet, K., and Luyben, K.Ch.A.M., (1989), "Estimation of axial dispersion in individual sections of an airlift-loop reactor", Chem. Eng. Sci., 44: 1139-1146.

[18] Wongsuchoto, P., (2002), "Bubble Characteristics and liquid circulation in internal loop airlift contractors", Ph.D. thesis, Faculty of Engineering, Chulalongkorn University, Thailand.

[19] Yu Wei, Wang Tiefeng, Liu Malin and Wang Zhanwen, (2008), "Bubble circulation regimes in a multi-stage internal-loop airlift reactor", Chemical Engineering Journal, 142, 301–308.

[20] Zhonghuo Deng, Tiefeng Wang, Nian Zhang, and Zhanwen Wang, (2010), "Gas holdup, bubble behavior and mass transfer in a 5m high internal-loop airlift reactor with non-Newtonian fluid", Chemical Engineering Journal, 160, 729–737.

[21] Znad H., V. Bales, and Y. Kawase, (2004), "Modeling and scale up of airlift bioreactor", Computers and Chemical Engineering, 28, 2765–2777.

محاكاة انتقال الاوكسجين في مفاعل Airlift ذو حقة الخلط الداخلي باستعمال موديل التشتت المحوري

محمد عبد عطية السراج* اميل محمد رحمن اسيل عبد الجبار****

وزارة التعليم العالي والبحث العلمي / دائرة البحث والتطوير

***قسم الهندسة الكيميائية الاحيائية/ كلية الهندسه الخوارزمي/ جامعة بغداد*

الخلاصة

تمت دراسة تاثير سرعة الغاز الفراغية ضمن المدى ٠.٠١-٠.١٦٤ م/ثا على الغاز المعلق (overall, riser and downcomer)، معامل انتقال الاوكسجين الحجمي، سرعة تدوير السائل في مفاعل من نوع airlift ذو الانبوبين المتمركزين داخليا بحجم كلي مقداره ٤٥ لتر. لوحظ عند زيادة سرعة الغاز الفراغية يزداد الغاز المعلق الكلي وزيادة سرعة تدوير السائل. ايضا وجد ان زيادة سرعة الغاز الفراغية تؤدي الى زيادة المساحة البينية التي تزيد معامل انتقال الاوكسجين الحجمي الكلي.

تم معاملة بيانات دراسة الهيدرودينمك بالعلاقات الرياضية المتوفرة بالادبيات. اظهرت البيانات المستحصلة من هذه العلاقات تطابقها بدقة عالية مع البيانات العلمية.

تم اعتماد تلك البيانات المستحصلة من العلاقات الرياضية وبيانات الجانب العملي في الموديل الرياضي لانتقال الاوكسجين لمعرفة مدى دقة الموديل الرياضي في وصف النظام المقترح. ان نتائج المحاكاة بالاعتماد على موديل التشتت للجزء riser و downcomer من المفاعل وموديل الخلط المثالي لجزء المفاعل الخاص بفصل الغاز عن السائل، تطابقها بشكل كبير مع النتائج العلمية ضمن مديات الظروف التشغيلية المدروسة.